INTELLIGENT AUTOLANDING CONTROLLER BASED ON NEURAL NETWOLKS

S. M. B. Malaek[1], Hojjat Izadi[2], Mehrdad Pakmehr[3]

[1] Associate Professor of Aerospace Engineering
Aerospace Engineering Department, Sharif University of Technology, Azadi Ave, Tehran, I.R. IRAN, P.O. Box: 11365-8639, Email: malaek@sharif.edu
[2] Graduate Student, Mechanical Engineering Department, Tarbiyat Modarres University All-e-Ahmad Highway, Tehran, Iran, Email: Izadi_hojjat@yahoo.com
[3] Graduate Student, Mechanical Engineering Department, Concordia University, Room H-549, 1455 de Maisonneuve Blvd. West, Montreal, QC, H3G 1M8, Canada, Email: MPakmehr@me.concordia.ca

Abstract: To expand the flight envelope of a typical jet transport and to minimize number of tests for the certification process, a design methodology has been proposed based on neural networks. The design procedure leads to an intelligent neuro-controller for landing phase that can handle different wind patterns. The procedure uses, a classical PID controller as the teaching mechanism of a neuro-controller. Finally, a hybrid neuro-PID controller which its inner loop is PID-based and its outer loop is neural-based has been proposed. Two wind patterns, *Strong* and *Very Strong* winds in comparison to JFK Airport Downburst, have been investigated to test the performance of the proposed controllers. To discuss the complexity of the controllers, three aspects have been considered. Simulation results show that the hybrid controller provides the necessary performance conditions in presence of Very Strong wind.

Keywords: Intelligent Controller, Neural Networks, Autolanding, Flight Safety Envelope, Atmospheric Conditions.

1. NOMENCLATURE

u	: perturbed longitudinal velocity (ft/sec.)
w	: perturbed vertical velocity (ft/sec.)
q	: perturbed pitch rate (deg/sec.)
θ	: perturbed pitch angle (deg.)
x	: horizontal position of aircraft (ft)
h	: altitude (ft)
$\dot{h}$	: sink rate (fps)
h_{0f}	: flare initiation altitude (ft)
g	: gravity (32.2 ft/sec^2)
u_g	: longitudinal wind velocity (ft/sec.)
w_g	: vertical wind velocity (ft/sec.)
δ_E	: elevator angle setting (deg.)
δ_T	: throttle setting (deg.)
U_0	: normal speed (235 ft/sec.)
γ_0	: flight path angle (-3 deg.)
h_{0g}	: glide initiation altitude (ft)
α_s	: stall angle of attack (deg.)

2. INTRODUCTION

Strong downbursts such as the one shown in Fig. 1 are responsible for number of hard landing and crash each year (Shen et al., 1996). Many research activities have been conducted to design an automatic landing controller for different classes of aircraft, especially heavy jet transports. For example, Ref. (Iiguni et al., 1998) describes an automatic landing system (ALS) based on a human skill model. The model is expressed as a nonlinear I/O mapping from the aircraft state to the control command provided by a human expert; a gain adaptation technique has also been introduced for robustness. In Ref. (Shue et al., 1999), a mixed H_2/H_∞ control technique has been employed to develop controllers for automatic landing system of a commercial airplane. In Ref. (Kaminer et al., 1990),

H_∞ synthesis has been applied to the problem of designing a flare mode for automatic landing for a typical transport airplane. In Ref. (Ben Ghalia et al., 1993), Linear Quadratic Gaussian with Loop Transfer Recovery (LQG/LTR) has been used to design an automatic landing controller for a typical commercial aircraft encountering a wind shear. In Ref. (Saini et al., 1997), adaptive critic neural networks have been used to design a controller for a benchmark problem in aircraft autolanding. In Ref. (Juang et al., 2001), five different neural network structures are utilized to design intelligent autolanding controllers using linearized inverse dynamic model. In Ref. (Yan et al., 2001), a Radial Basis Function Neural Network (RBFN) has been used in the control scheme to aid a conventional controller for aircraft autolanding procedure. In Ref. (Kee et al., 2001), a controller based on fuzzy logic methodology has been designed for a flight vehicle that enables it to track a pre-determined flight path trajectory for safe landing. All of these works suffer from the point that they lack sufficient generality for a flight phase as landing phase is. Landing as a flight phase which normally has the highest percentage of accidents and/or incident could vary considerably (Jeppesen Inc., *Private Pilot Manual*, 1992) due to its vicinity to the ground and existence of unknown pattern of wind and gust in addition to the other factors surrounding an airport. It is therefore desirable to develop a control system that can handle different climatic conditions and in this regard, neuro based control systems could be a solution.

Accidents during the landing phase could fall into two different categories. The first category is related to the human errors and the second one is due to the sudden changes in atmospheric conditions. It is the intention of this work to present a methodology to practically, omit the need for switching between glide and flare modes during landing phase of flight in presence of very strong winds with the help of neural networks technique. The procedure has three major steps as follows:

a. Firstly, a PID controller is designed for a known trajectory.
b. Secondly, a neuro-controller is designed to control the aircraft through-out the glide and flare modes.
c. Finally a hybrid neuro-PID controller is designed to handle the aircraft in Very Strong wind pattern. In this controller the inner loop is PID based and the outer loop is neural based.

In this approach, the data and outputs generated by the PID controller are used to train the neuro-controller. Obviously, the PID controller is deigned only for a single known trajectory in a specific set of conditions. However, it could be used for a wide range of flight conditions, based on the characteristics of neural networks. Omission of the switching mechanism between the glide and flare modes leaves out the selection of proper point to flare. In this way, uncertainties due to the so called "sensor errors" are no longer a concern. Different simulation conducted shows that with the help of hybrid neuro-PID technique acceptable landing performance in severe atmospheric conditions are possible.

3. PROBLEM DEFINITION AND OBJECTIVES

During complex manoeuvres, such as landing and take-off; the dynamics of the aircraft is changing rapidly which leads to a complex design procedure as far as conventional controllers are concerned. The problem can become even more complex, while gusts and other natural climatic conditions are present. Two major modes of landing phase studied here are glide-slope hold and intercept and flare and touch down with regard to (Roskam, 1979). The following characteristics are usually observed, during landing phase of a flight:

1. A suitable altitude should be selected for the aircraft autopilot to start to glide mode or glide mode initiation.
2. At a height of about 15 meters (45 ft) AGL, the flare manoeuvre is started which results in nose being lifted, reducing the vertical speed of the aircraft and allowing the main gear to touch the ground firstly and smoothly. During this limited time interval the control law has to be adjusted continuously.
3. Through continuous decrease in the aircraft altitude, the ground effect starts to play a major role and the aircraft dynamics becomes affected accordingly.
4. Gust and downburst, which have an inevitable influence on the aircraft dynamics, do not follow a well-known pattern.

Based on design performance outlined in (Hueschen, 1986 a), (Hueschen, 1986 b) and (Heffley et al., 1982), it is desired to have controllers to satisfy the following conditions:

$$|\dot{h}| \le 20 \ fps \qquad (*)$$

$$|\theta| \le 20 \deg \qquad (**)$$

$$|\alpha| \le 10 \deg \qquad (***)$$

It is further assumed that glide mode begins at 500 ft AGL and finishes at 45 ft AGL, which is the start point of flare mode (Roskam, 1979) (Fig. 2). The flare mode continues until a smooth touch down is achieved. During a glide-slope mode, an automatic landing system guides the aircraft along a straight line with a constant slope (with a constant glide angle, γ). Autopilot also attempts to prevent any changes in aircraft vertical and horizontal speeds, that is, during glide mode the sink rate is constant.

As flare mode starts, autopilot starts to nose up the aircraft by changing the glide angle to prepare aircraft for a smooth touchdown. The trajectory of aircraft during this mode is estimated by an exponential function. Through this mode the sink rate is reduced to the desired value of -1.5 fps. A longitudinal control surface such as elevator in addition to the throttle is the usual control during these modes.

4. AIRCRAFT EQUATIONS OF MOTION AND TURBULANCE MODEL

In this work, 3-DOF equations of motion in the vertical plane known as longitudinal dynamics have been used to design the controller, however, the procedure is very well extendable to a complete 6-DOF equations of motion. Based on (Roskam, 1979), these equations are given by (1) through (9).

$$\dot{u} = X_u(u-u_g) + X_w(w-w_g) + X_q q - g\left(\frac{\pi}{180}\right)\cos(\gamma_0)\theta + X_E\delta_E + X_T\delta_T \quad (1)$$

$$\dot{w} = Z_u(u-u_g) + Z_w(w-w_g) + \left(Z_q - \left(\frac{\pi}{180}\right)U_0\right)q + g\left(\frac{\pi}{180}\right)\sin(\gamma_0)\theta + Z_E\delta_E + Z_T\delta_T \quad (2)$$

$$\dot{q} = M_u(u-u_g) + M_w(w-w_g) + M_q q + M_E\delta_E + M_T\delta_T \quad (3)$$

$$\dot{\theta} = q \quad (4)$$

$$\dot{x} = u\cos\theta + w\sin\theta \quad (5)$$

$$\dot{h} = u\sin\theta - w\cos\theta \quad (6)$$

The initial conditions are assumed as:

$$u(0)=w(0)=q(0)=\theta(0)=0 \quad (7)$$

$$h(0)=500 \text{ ft}, \; x(0)=h(0)/\text{tg}\,\gamma_0 \quad (8)$$

$$\dot{x}(0) = U_0 \quad (9)$$

Wind disturbance, which are shown by (u_g, w_g) consists of two components: constant velocity (u_{gc}, 0) and turbulence (u_{g1},w_g). It is further assumed that the constant velocity component exists only in the horizontal direction, given by (10),

$$u_{gc} = \begin{cases} -u_0(1+\text{Ln}(h/510)/\text{Ln}51) & h \geq 10 \\ 0 & h < 10 \end{cases} \quad (10)$$

Here u_0 is the wind speed at altitude 510 ft and its typical value is 20 ft/sec. Turbulence is represented by (Iiguni et al., 1998).

$$u_g = u_{g1} + u_{gc} \quad (11)$$

$$w_g = \sigma_w\sqrt{a_w}(a_w w_{g_1} + \sqrt{3}w_{g_2}) \quad (12)$$

$$\dot{u}_{g_1} = 0.2|u_{g_c}|\sqrt{2a_u}N_1 - a_u u_{g_1} \quad (13)$$

$$\dot{w}_{g_1} = w_{g_2} \quad (14)$$

$$\dot{w}_{g_2} = N_2 - a_w^2 w_{g_1} - 2a_w w_{g_2} \quad (15)$$

Where

$$a_u \begin{cases} U_0/(100\sqrt[3]{h}) & ; h > 230 \\ U_0/600 & ; h \leq 230 \end{cases} \quad (16)$$

$$a_w = U_0/h \quad (17)$$

$$\sigma_w \begin{cases} 0.2|u_{gc}|; & h > 500 \\ 0.2|u_{gc}|(0.5+0.00098\,h); & h \leq 500 \end{cases} \quad (18)$$

And N_1 and N_2 are the Gaussian Random Noises with mean zero and different variances. In this approach means, wind patterns with different velocities and intensities can be generated.

5. AUTOLAND CONTROLLER DESIGN

As previously mentioned, a conventional PID controller, a modern neuro-controller and also a hybrid neuro-PID controller are designed to show the effectiveness of a hybrid system. To design a PID controller to train the Neuro-controller, longitudinal controls are *throttle* and *elevator*. Throttle is used in such a way that the aircraft speed during landing phase remains constant (Iiguni ET AL., 1998). So:

$$T = K_T(u_c - u) + K_T\omega_T\int_0^t (u_c - u)dt \quad (19)$$

In this case: u_c= 0, k_T= 3, w_T= 0.1.

The function of elevator is to control the pitch angle and pitch rate during landing phase, so:

$$E = K_\theta(\theta_c - \theta) - K_q q \quad (20)$$

And it is further assumed that, the desired pitch angle is a function of error in h and $\dot{h}$, so

$$\theta_c = k_h(h_c - h) + k_h\omega_h\int_0^t (h_c - h)dt + k_{\dot{h}}(\dot{h}_c - \dot{h}) + \theta_p \quad (21)$$

Where

K_h=0.3, W_h=0.1, $K_{\dot{h}}$ =0.3

At *Glide* mode: $K_\theta = 3$, K_q=3, $\theta_p = 0$

At *Flare* mode: $K_\theta = 12$, K_q=6.0, $\theta_p = 0.0698$

The PID controller gains are estimated by applying the Linear Matrix Inequality (LMI) method, which is normally used to design PID controllers for MIMO systems. This method guarantees the stability of the designed system (Zheng et al., 2002). However, to achieve the desired performance one needs to optimize the gains through a trial and error process.

h_c and $\dot{h}_c$ for each mode are obtained from their trajectories in glide and flare modes. As we know in glide mode the aircraft moves along a constant slope path characterized by (22):

$$tg\gamma_0 = \frac{h_c}{x} \quad \Rightarrow \quad h_c = x\,tg\gamma_0 \quad (22)$$

At the flare mode the controller is applied to aircraft so that $\dot{h}$ is reduced smoothly to a desired value of -1.5 fps. It is assumed that the flare mode begins at $t=t_0$ and $h_{0f}=h(t_0)$=45 ft and it ends at the main gear touch down point where t=T and h(T)=0, then:

$$h_c = \frac{h_0}{\dot{h}_0 - \dot{h}_T}(\dot{h}_0 e^{-(x-x_0)\tau} - \dot{h}_{TD}) \quad (23)$$

Where

$$\dot{h}_{TD} = \dot{h}(\tau) = -1.5(ft/\text{sec}) \quad (24)$$

$$\tau = [-h_0\,x(t_0)]/(\dot{h}_0 - \dot{h}_T) \quad (25)$$

Results of different simulations conducted by the authors show that setting the throttle command to zero results in much better trajectories. Therefore, the rest of the simulations, once the throttle setting was selected it was treated as a constant throughout the simulation.

6. NEURO-CONTROLLER DESIGN

One neural network is designed for Elevator control. As previously mentioned the outputs of PID controller are used to train the neural network. The neural network used for Elevator control is a Multi Layer Perceptron (MLP) with the name of *elevatornet*, which has 3 layers and 4 inputs (θ, q, h and $\dot{h}$). The output of elevatornet is the elevator

setting. The hidden layer has 7 neurons ($N_{4,7,1}$). In this neural network, tangent-sigmoid function is used in input and hidden layers and pure-linear function is used in output layers. To train the network classical *error back propagation method* (*Levenberg-Marquardt back propagation*) is used. This method updates weight and bias values according to Levenberg-Marquardt optimization (Demuth et al, 2000).

7. HYBRID NEURO-PID CONTROLLER DESIGN

To achieve a better performance in the presence of very strong winds and gusts a new controller has been proposed. In this controller inner loop that provides stability of the system, is designed with the aid of classic methods (such as root locus plot), in other words, according to equations for elevator setting (20), we tune K_θ and K_q by classical methods. The outer loop (θ_c) is estimated by a type of neural networks named General Regression Neural Networks (GRNN). A GRNN is often used for function approximation and has a radial basis layer as it hidden layer and a special linear layer as its output layer (Demuth et al, 2000).

8. CASE STUDIES AND SIMULATION RESULTS

To train the networks, the M-files and Neural Networks Toolbox (Demuth et al, 2000) of Matlab software have been used, and to simulate the system, Simulink Toolbox (Simulink Toolbox User's Guide, 2000) of Matlab software has been used; also, suitable links between the M-files and Simulink environment have been provided. The initial conditions for all of the aforementioned controllers have been introduced in Equations (7) to (9).

According to FAR 25 Federal Aviation Administration regulations (FAA AC20-57A, 1971), environmental conditions considered in the determination of dispersion limits are: headwinds up to 25 knots (42.23 fps); tailwinds up to 10 knots (16.9 fps). The simulation result of the designed hybrid controller was found to be robust enough to properly handle all of the imposed turbulences proposed by the FAA in landing phase of flight.

Fig. 3 to 6, show the horizontal and vertical components of *Strong* and *Very Strong* winds applied to the controllers. Simulation results have been presented separately for the Strong wind and Very Strong wind. The profiles of strong wind are depicted in Fig. 3 and 4. And the simulation results for this wind have been shown in Fig. 7 to 12. Followed and commanded trajectories of aircraft for all of three controllers are shown in Fig. 7 to 9. It is observed that for all of controllers have acceptable performances. The sink rate variations for the controllers are shown in Fig. 10 to 12, which all of them satisfy the requested performance (*). It is observed that the variations of angles of attack for all of the cases are in the acceptable range, with regard to angle of attack limitation (Stall angle, α_s) (***). Consequently, all of the controllers- PID, Neuro, and Neuro-PID controller- have good capabilities to guide the aircraft throughout the landing phase in presence of Strong wind.

Horizontal and vertical components of Very Strong wind have been depicted in Fig. 5 and 6. Comparing these figures with JFK Airport Downburst, Fig. 1, it is seen that the wind named Very Strong wind is stronger than the JFK Airport Downburst. Fig. 13 to 18, show simulation results of the controllers in presence of Very Strong wind. Followed and commanded trajectories for the controllers, in presence of Very Strong wind, have been shown in Fig. 13 to 15. Fig. 13 shows that the classic controller follows the commanded trajectory well, but according to Fig. 14, the neuro controller does not have an acceptable behaviour, while following the commanded trajectory. Fig. 15 shows that the neuro-PID controller has a relative better performance.

Desired and actual sink rates for the controllers have been shown in Fig. 16 to 18. Actual sink rate of classic controller (Fig. 16) exceeds -20 fps and does not satisfy the conditions (*). The neuro controller also does not satisfy the limitations in this case (Fig. 17). Sink rate of the aircraft with hybrid neuro-PID controller (Fig. 18) in presence of Very Strong wind does not exceed -20 fps limitation and satisfies the conditions (*). Variation of angle of attack with neuro controller is not acceptable. Angle of attack of the aircraft in presence of Very Strong wind, with applying the PID and neuro-PID controllers does not exceed the stall angle limitation (***), during the landing phase of flight, but neuro-PID controller has a relative better performance. The aforementioned results have been shown in Table 1:

Table 1: Performance of the controllers in presence of different wind patterns

controller / wind pattern	**PID Controller**	**Neuro Controller**	**Neuro-PID Controller**
Strong	Acceptable	Acceptable	*Acceptable*
Very Strong	Unacceptable	Unacceptable	*Acceptable*

9. DISCUSSION AND CONCLUSION

Three different types of controllers (Classic, Neuro, and Neuro-PID) have been designed and simulated. To evaluate performance of the controllers, two different wind patterns have been introduced, named Strong and Very Strong winds. Strong wind is weaker than the JFK Downburst and Very Strong wind is stronger than it. Results show that performance of controllers in presence of Strong wind is acceptable. But, only the hybrid neuro-PID controller behaves well in presence of Very Strong wind pattern. So only with applying the hybrid neuro-PID controller we can extend the flight envelop of the aircraft.

Complexity of the controllers could be discussed from three different aspects: 1- Number of required sensors. 2- Amount of required computations and calculations. 3- Required switching.

Block diagrams of the PID, neuro and neuro-PID controllers have been shown consequently in Fig. 18 to 21. As it is obvious, $\theta, q, h \text{ and } \dot{h}$ are the inputs of

the controllers, so the number of required sensors for all of the controllers is equal. From the second point of view, the neuro-PID controller because of so many processing units of the GRNN network, performs a great amount of calculations, but this is not a negative point for the neuro-PID controller, since the overall time which is needed to generate the trajectory by the neuro-PID controller in comparison with the time which is needed by the aircraft to fulfil its mission, is negligible and this set of calculations can be done with the aid of new computers. From the third point of view, the only controller which does not need any switching is neuro controller.

It can be seen from the previous section that the PID controller needs different gains in glide slope and flare modes and this causes switching between these two modes. This switching generates some problems with the controller. For example; the switching needs the exact information of sensors to switch between these two modes and it is obvious that the PID controller needs precise measurements of sensors near the run way, while it is known that the sensors have some errors. In addition, switching also generates some noises in electronic systems of controller.

On the other hand, the neuro-controller has a good ability to estimate the system parameters in a condition that had not been trained before, and to extend the performance range of the system. In other words by this technique the flight envelope of the aircraft can be extended in a wide range and this make the landing system operate more safely in presence of sudden and unpredicted conditions and it is possible to decrease the number of flight tests. In overall, a mixed Neuro-Classic controller has a better performance in comparison with the controllers which are based only on classic methods or only on neural networks methods.

REFERENCES

Ben Ghalia Mounir, Alouani Ali T., "*Robust Control Design of an Autolanding System*", IEEE Conference, 1993.

Demuth H., Beale M., *Neural Networks Toolbox (For Use with Matlab) User's Guide*, Version 4, Mathworks Inc., 2000.

Federal Aviation Administration (FAA), "*Automatic Landing Systems*", AC 20-57A, Jan. 1971.

Heffley R. K., Schulman T. M., Clement W. F., "*An Analysis of Airline Landing Flare Data Based on Flight and Training Simulator Measurements*", NASA-CR-166404, NASA National Aeronautics and Space Administration, Ames Research Centre, August 1982.

Hueschen Richard M., "*Implementation and flight tests for the Digital Integrated Automatic Landing System (DIALS), Part 1*", NASA-TM-87632-PT-1, NASA National Aeronautics and Space Administration, Langley Research Centre, July 1986.

Hueschen Richard M., "*Implementation and flight tests for the Digital Integrated Automatic Landing System (DIALS), Part 2*", NASA-TM-87632-PT-2, NASA National Aeronautics and Space Administration, Langley Research Centre, July 1986.

Iiguni Youji, Akiyoshi Hideo, Adachi Norihiko, "*An Intelligent Landing System Based on a Human Skill Model*", *IEEE Transactions on Aerospace and Electronic Systems*, **Vol. 34**, No.3, July 1998.

Jeppesen Sanderson Inc., *Private Pilot Manual*, 1992.

Juang Jih-Gau, Chang Hao-Hsiang, Cheng Kai-Chung, "*Intelligent Landing Control Using Linearized Inverse Aircraft Model*", American Control Conference, Vol. 4, 2001, PP 3269-3274.

Kaminer Issac, Khargonekar Pramod P., "*Design of the Flare Control Law for longitudinal Autopilot Using* H^{∞} *Synthesis*", Proceedings of the 29th Conference on Decision and Control, Honolulu, Hawell, IEEE 1990.

Kee P. E., Dong L., "*Fuzzy-Logic Based Autoland Controller*", can be downloaded from: http://www.mindef.gov.sg/rsaf/ats2002/uav/Uv3.pdf.

Martens D., "*Neural Networks as a Tool for the Assessment of Human Pilot Behaviour in Wind Shear*", Aerospace Science and Technology, No.1, 1999, Page: 39–48.

Roskam J.., *Airplane Flight Dynamics and Automatic Flight Control (Part I & II)*, Roskam Publishing Incorp., 1979.

Saini Gaurav, Balakrishnan S. N., "*Adaptive Critic Based Neuro-Controller for Autolanding of Aircraft*", Proceedings of the American Control Conference, Albuquerque, New Mexico, June 1997.

Shen J., Park E. K., Bach R. E., "*Comprehensive Analysis of Two Downburst-Related Aircraft Accidents*", *Journal of Aircraft*, **Vol. 33**, No. 5, PP. 924-930, 1996.

Shue Shgh-Pyng, Agrawal Ramesh K., "*Design of Automatic Landing Using Mixed* H_2/H_∞ *Control*", *Journal of Guidance, Control & Dynamics*, **Vol. 22**, No.1, January-February 1999.

Simulink Toolbox of Matlab (Model-Based and System-Based Design) User's Guide, Version 4, Mathworks Inc., 2000.

Yan L., Sundararajan N., Saratchandran P., "*An Investigation of a Neuro-Controller in Automatic Landing*", can be downloaded from: http://www.mindef.gov.sg/rsaf/ats2002/uav/Uv4.pdf.

Zheng Feng, Wang Qing-Guo, Lee Tong Heng, "*Brief Paper on the Design of Multivariable PID Controllers via LMI Approach*", *Journal of Automatica*, **Vol. 38**, 2002, PP 517-526.

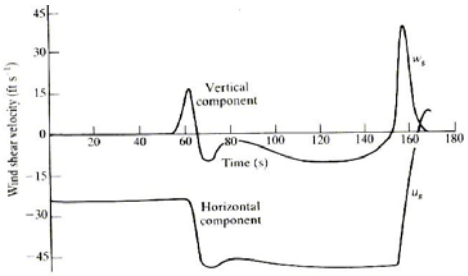

Fig. 1: JFK Airport Downburst

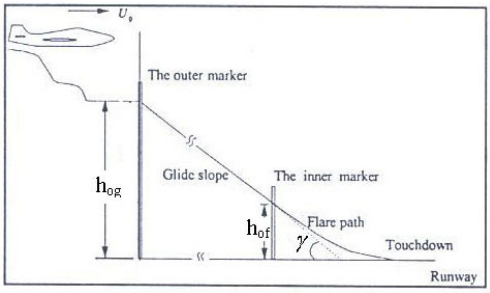

Fig. 2: Typical trajectory in landing

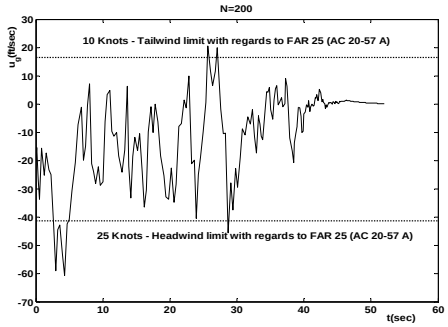

Fig. 3: Strong wind pattern, Variation of u_g with h, N=200

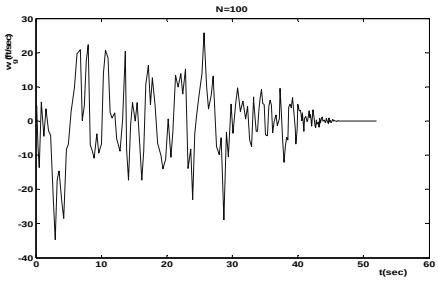

Fig. 4: Strong wind Pattern, Variation of w_g with h, N=100

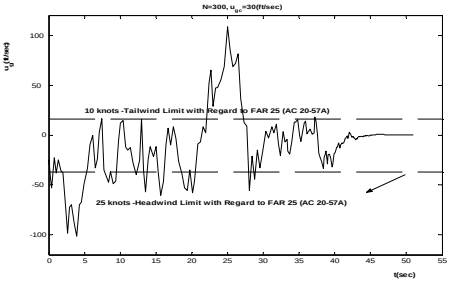

Fig. 5: Very Strong wind pattern, Variation of u_g with h, N=300

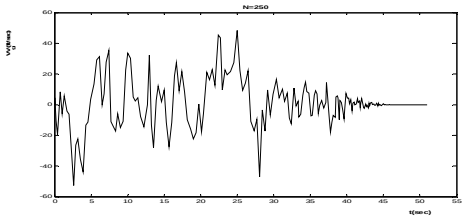

Fig. 6: Very Strong wind Pattern, Variation of w_g with h, N=250

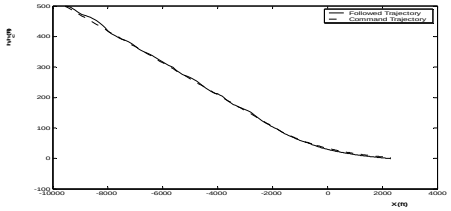

Fig. 7: Trajectory for PID controller with Strong wind

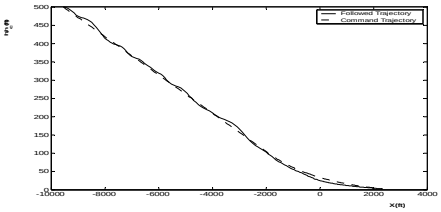

Fig. 8: Trajectory for Neuro controller with Strong wind

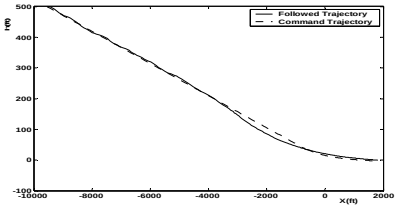

Fig. 9: Trajectory for Neuro-PID controller with Strong wind

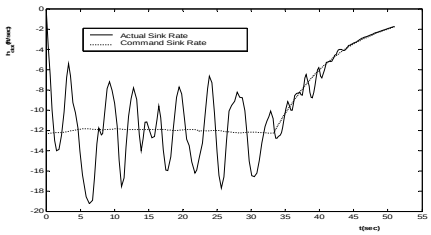

Fig. 10: Sink rate variations for PID controller with Strong wind

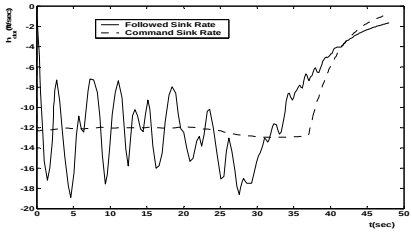

Fig. 11: Sink rate variations for Neuro controller with Strong wind

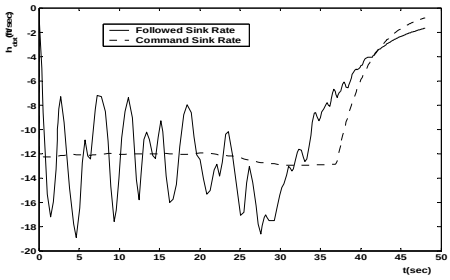

Fig. 12: Sink rate variations for Neuro-PID controller with Strong wind

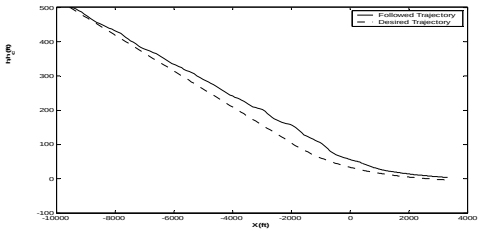

Fig. 13: Trajectory for PID controller with Very Strong wind

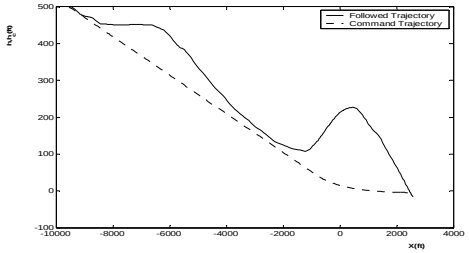

Fig. 14: Trajectory for Neuro controller with Very Strong wind

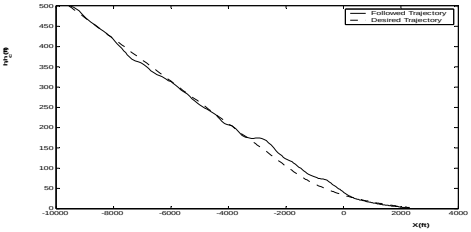

Fig. 15: Trajectory for Neuro-PID controller with Very Strong wind

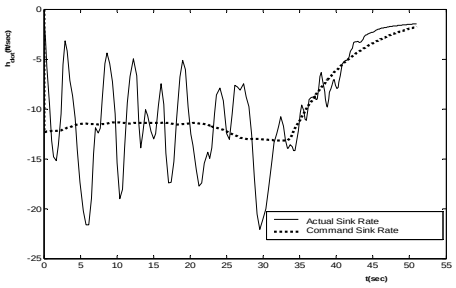

Fig. 16: Sink rate variations for PID controller with Very Strong wind

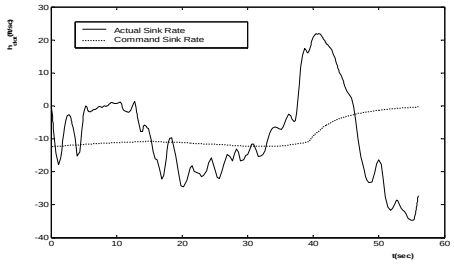

Fig. 17: Sink rate variations for Neuro controller with Very Strong wind

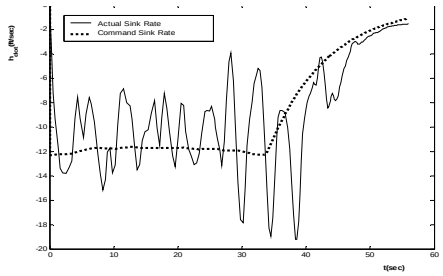

Fig. 18: Sink rate variations for Neuro-PID controller with Very Strong wind

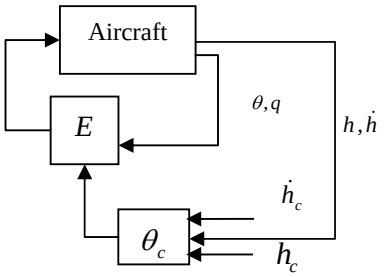

Fig. 19: PID Controller block diagram

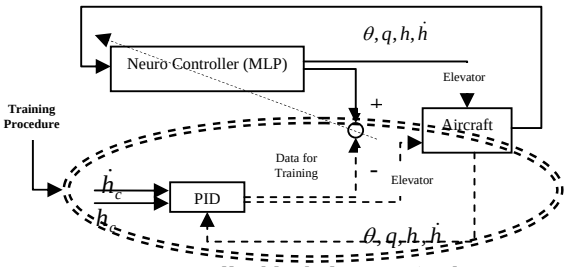

Fig. 20: Neuro Controller block diagram (with training procedure)

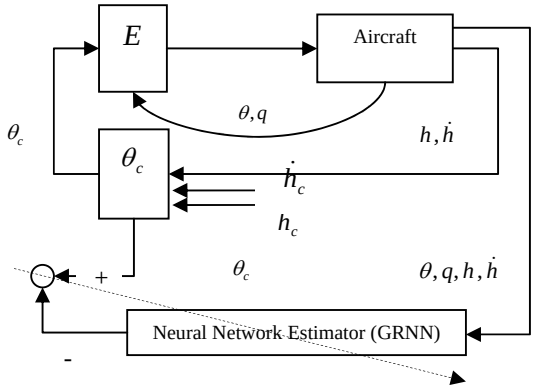

Fig. 21: Neuro-PID Controller block diagram (with training procedure**)**